



# Aerospace Ceramic Materials: Thermal, Environmental Barrier Coatings and SiC/SiC Ceramic Matrix Composites For Turbine Engine Applications

*Dongming Zhu*  
*Glenn Research Center, Cleveland, Ohio*

## NASA STI Program . . . in Profile

Since its founding, NASA has been dedicated to the advancement of aeronautics and space science. The NASA Scientific and Technical Information (STI) Program plays a key part in helping NASA maintain this important role.

The NASA STI Program operates under the auspices of the Agency Chief Information Officer. It collects, organizes, provides for archiving, and disseminates NASA's STI. The NASA STI Program provides access to the NASA Technical Report Server—Registered (NTRS Reg) and NASA Technical Report Server—Public (NTRS) thus providing one of the largest collections of aeronautical and space science STI in the world. Results are published in both non-NASA channels and by NASA in the NASA STI Report Series, which includes the following report types:

- TECHNICAL PUBLICATION. Reports of completed research or a major significant phase of research that present the results of NASA programs and include extensive data or theoretical analysis. Includes compilations of significant scientific and technical data and information deemed to be of continuing reference value. NASA counter-part of peer-reviewed formal professional papers, but has less stringent limitations on manuscript length and extent of graphic presentations.
- TECHNICAL MEMORANDUM. Scientific and technical findings that are preliminary or of specialized interest, e.g., “quick-release” reports, working papers, and bibliographies that contain minimal annotation. Does not contain extensive analysis.
- CONTRACTOR REPORT. Scientific and technical findings by NASA-sponsored contractors and grantees.
- CONFERENCE PUBLICATION. Collected papers from scientific and technical conferences, symposia, seminars, or other meetings sponsored or co-sponsored by NASA.
- SPECIAL PUBLICATION. Scientific, technical, or historical information from NASA programs, projects, and missions, often concerned with subjects having substantial public interest.
- TECHNICAL TRANSLATION. English-language translations of foreign scientific and technical material pertinent to NASA's mission.

For more information about the NASA STI program, see the following:

- Access the NASA STI program home page at <http://www.sti.nasa.gov>
- E-mail your question to [help@sti.nasa.gov](mailto:help@sti.nasa.gov)
- Fax your question to the NASA STI Information Desk at 757-864-6500
- Telephone the NASA STI Information Desk at 757-864-9658
- Write to:  
NASA STI Program  
Mail Stop 148  
NASA Langley Research Center  
Hampton, VA 23681-2199

NASA/TM—2018-219884



# Aerospace Ceramic Materials: Thermal, Environmental Barrier Coatings and SiC/SiC Ceramic Matrix Composites For Turbine Engine Applications

*Dongming Zhu*  
*Glenn Research Center, Cleveland, Ohio*

National Aeronautics and  
Space Administration

Glenn Research Center  
Cleveland, Ohio 44135

---

May 2018

## Acknowledgments

The author are specifically grateful to Dr. James L. Smialek and Dr. James A. DiCarlo (retired), both Senior Technologists at NASA Glenn Research Center, for helpful discussions and reviewing this Ceramic Materials Section paper. Much of the NASA Glenn Research Center related ceramic material development in this review was supported by NASA Aeronautics Programs. Especially most recently by the NASA Transformational Tools and Technologies Project. The author would like to thank Janet B. Hurst and Dale Hopkins, for the program supports of the development of ceramic environmental barrier coatings and SiC/SiC ceramic matrix composites. The author also expresses his gratitude to Dr. Biliyar N. Bhat, NASA Marshall Space Flight Center, for helpful discussions and particularly his guidance in the section topic contents.

This work was sponsored by the  
Transformative Aeronautics Concepts Program.

*Level of Review:* This material has been technically reviewed by technical management.

Available from

NASA STI Program  
Mail Stop 148  
NASA Langley Research Center  
Hampton, VA 23681-2199

National Technical Information Service  
5285 Port Royal Road  
Springfield, VA 22161  
703-605-6000

This report is available in electronic form at <http://www.sti.nasa.gov/> and <http://ntrs.nasa.gov/>

# **Aerospace Ceramic Materials: Thermal, Environmental Barrier Coatings and SiC/SiC Ceramic Matrix Composites For Turbine Engine Applications**

Dongming Zhu  
National Aeronautics and Space Administration  
Glenn Research Center  
Cleveland, Ohio 44135

## **Abstract**

Ceramic materials play increasingly important roles in aerospace applications because ceramics have unique properties, including high temperature capability, high stiffness and strengths, and excellent oxidation and corrosion resistance. Ceramic materials also generally have lower densities as compared to metallic materials, making them excellent candidates for light-weight hot-section components of aircraft turbine engines, rocket exhaust nozzles, and thermal protection systems for space vehicles when they are being used for high-temperature and ultra-high temperature ceramics applications. Ceramic matrix composites (CMCs), including non-oxide and oxide CMCs, are also recently being incorporated in gas turbine engines for high pressure and high temperature section components and exhaust nozzles. However, the complexity and variability of aerospace ceramic processing methods, compositions and microstructures, the relatively low fracture toughness of the ceramic materials, still remain the challenging factors for ceramic component design, validation, life prediction, and thus broader applications.

This ceramic material section paper presents an overview of aerospace ceramic materials and their characteristics. A particular emphasis has been placed on high technology readiness level (TRL) enabling ceramic systems, that is, turbine engine thermal and environmental barrier coating systems and non-oxide type SiC/SiC CMCs. The current status and future trend of thermal and environmental barrier coatings and SiC/SiC CMC development and applications are described.

## **Introduction**

Ceramics are important materials for aerospace applications because of their high temperature capability (high melting point), high stiffness and strengths, and excellent resistance to oxidation and corrosion. Ceramic materials also generally have lower densities and thus higher specific strengths as compared to metallic materials. Currently used engineering or structural ceramics (a.k.a. crystalline inorganic non-metallic materials) in aerospace include ceramic thermal and environmental barrier coatings (EBCs) for protecting hot section components of aircraft turbine engines from high heat flux in high temperature combustion environments, rocket exhaust nozzles, and thermal protection systems for space vehicles. Ceramic matrix composites (CMCs), including non-oxide and oxide CMCs, are also being incorporated in turbine engines in high pressure and high temperature section components and turbine exhaust nozzles with long duration design operating lifetimes.

Although ceramic materials have many attributes that make them excellent materials for high temperature and ultra-high temperature protective coatings and structural materials, the current uses have been limited due to their low toughness, large variability in mechanical properties, and complex environmental effects in harsh operating conditions. The complexity and variability of aerospace ceramic

processing methods, compositions and microstructures also make the material design and validation a more challenging task.

This ceramic material section paper presents an overview of aerospace ceramic materials and their characteristics. The focus is on important enabling ceramic systems for aerospace applications, particularly turbine engine thermal and EBC systems: non-oxide type SiC/SiC CMCs. This section also covers the ceramic materials for various applications, material system properties and durability performance associated with processing, and thermal, thermomechanical, and environmental life design considerations. A brief discussion of laboratory and simulated operating environment tests is included.

The paper is divided into the following subsections: thermal barrier coatings, environmental barrier coatings, and particularly SiC/SiC ceramic matrix composites. Monolithic ceramics have limited fracture toughness, they are used as constituents of the ceramic surface coatings, ceramic matrices, fibers or fiber coatings, and therefore some of their pertinent properties are also described or compared with processed coatings or composites. In each of the subsections, a brief history and material system improvements will be presented. In the CMC section, the ceramic fiber attributes will also be briefly discussed. The current status and future trend of CMC development and applications are described.

## **Thermal Barrier Coatings**

The performance and efficiency of aero propulsion turbine engines are directly related to the operating temperatures. Ceramic thermal barrier coatings (TBCs) are technologically important because of their ability to increase turbine engine operating temperatures and reduce cooling requirements, thus help to achieve engine performance and emission goals (Refs. 1 to 10).

The advances in ceramic material and processing technologies, particularly for zirconia based ceramics, have resulted in the application of ceramic TBCs on air cooled, critical turbine engine hot-section components, such as combustors, high pressure turbine vanes and blades, as shown in Figure 1. Since the initial entry into commercial service in 1980s (Refs. 2 and 9), TBCs have achieved significant temperature benefits that are surpassing other materials including nickel based single crystal superalloys and cooling technology advances achieved in the last three decades (Refs. 6 and 9). TBCs have provided high pressure turbine (HPT) component metal temperature reduction up to 100 °C, and future potential greater than 200 °C reductions is expected (Ref. 9), particularly when more advanced low thermal conductivity coatings are incorporated.

Thermal barrier coatings are complex, two-layer or multilayered, multimaterial systems. A typical TBC system consists of a two layers: a ceramic zirconia ( $ZrO_2$ ) coating top coat, and a metallic bond coat (either NiCrAlY, NiCoCrAlY, CoNiCrAlY or PtAl) that are deposited on a nickel-based superalloy substrate. In addition, low diffusion and protective  $Al_2O_3$  scales, thermally grown oxide (TGO) on the TBC bond coat, are also critical for thermal barrier coating technology. The TGO scales, formed on the bond coats between the alloy bond coat and ceramic thermal barrier coatings, the bond coat temperatures, and its cyclic endurance, are important design parameters in determining the thermal barrier coating life (Ref. 11).

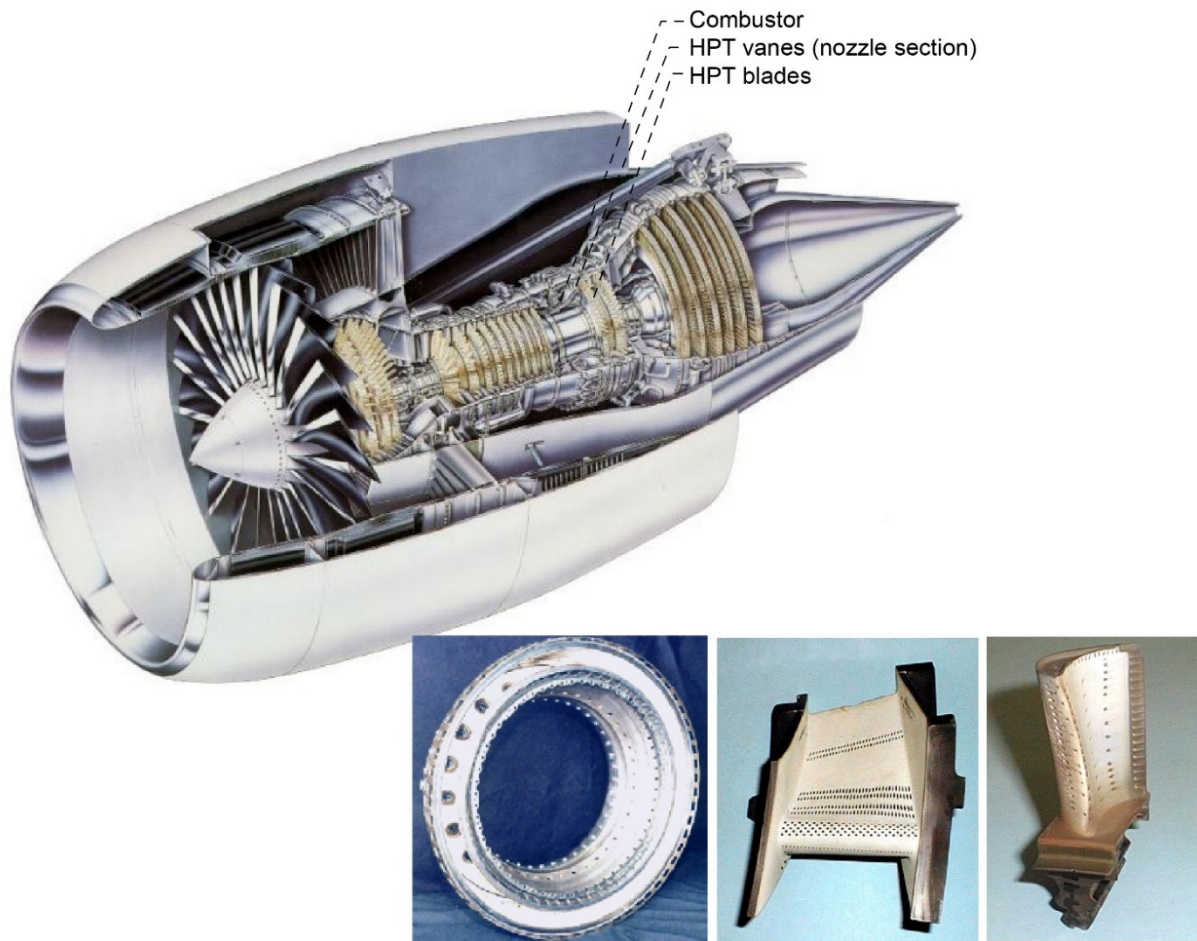


Figure 1.—A schematic diagram of a high bypass turbofan engine. Thermal barrier coatings are extensively used in the hot-section of turbine components, including combustors, high pressure turbine (HPT) vanes, and HPT blades (the inset pictures show examples of the thermal barrier coated turbine components).

TBCs and the material systems are processed and integrated using various processing methods, including commonly used plasma spray and electron beam – physical vapor deposition (EB-PVD). Other thermal spray processing methods such as suspension plasma spray (SPS) and plasma spray – physical vapor deposition (PS-PVD) are also being developed and used (Ref. 12). Turbine engine airfoil components (turbine vanes and blades) typically have thermal barrier coating thicknesses ranging from 100 to 250  $\mu\text{m}$ , whereas combustor or other non-rotating components have a coating thickness ranging from 250 to 500  $\mu\text{m}$ . The coating system compositions, microstructures and properties can greatly affect the coating durability during engine operations. Microstructures of plasma sprayed and EB-PVD thermal barrier coatings are shown in Figure 2. It can be seen that micro-cracks and porosity in the plasma sprayed splat type of coatings, with both intra-columnar and inter-columnar porosity in EB-PVD columnar coatings, are present in the microstructure, which help to increase the thermal strain tolerance and reduce the thermal conductivity of the coating systems.

Zirconia ( $\text{ZrO}_2$ ) is used for thermal barriers because it has a high melting point (approximately 2700  $^\circ\text{C}$ ), low intrinsic thermal conductivity (approximately 2.0 to 2.5  $\text{W/m-K}$ ), and relatively high coefficient of thermal expansion, and thus is an ideal ceramic material for protecting nickel based superalloy components for high temperature TBC applications. Oxide alloy dopants such as  $\text{Y}_2\text{O}_3$  or rare earth (RE) oxides (e.g.,  $\text{Yb}_2\text{O}_3$ ,  $\text{Gd}_2\text{O}_3$ ) are added to stabilize the zirconia and retain the high temperature phases,

particularly favorable metastable tetragonal phase structure, or cubic phase structure, which suppresses the detrimental martensitic tetragonal to monoclinic phase transformation during service (Refs. 13 and 14). The current state of the art  $ZrO_2 - (6 \text{ to } 8) \text{ wt\% } Y_2O_3$  TBC compositions have the metastable tetragonal ( $t'$ ) phase structures, which possesses high toughness and excellent cyclic durability (Refs. 9 and 15). NASA's early coating TBC development showed the best furnace cyclic life and durability for the TBC coating systems with a composition range of  $ZrO_2 - 6 \text{ to } 8 \text{ wt\% } Y_2O_3$ , as illustrated in Figure 3. The more recent work by Mercer et al. (Ref. 16) showed that the metastable tetragonal coating composition 7YSZ ( $ZrO_2 - 7 \text{ wt\% } Y_2O_3$ ) has a higher fracture toughness value ( $3.0 \text{ MPa m}^{0.5}$ ), compared to another commercially available higher  $Y_2O_3$  content TBC composition  $ZrO_2 - 20 \text{ wt\% } Y_2O_3$  ( $1.0 \text{ to } 1.2 \text{ MPa m}^{0.5}$ ).

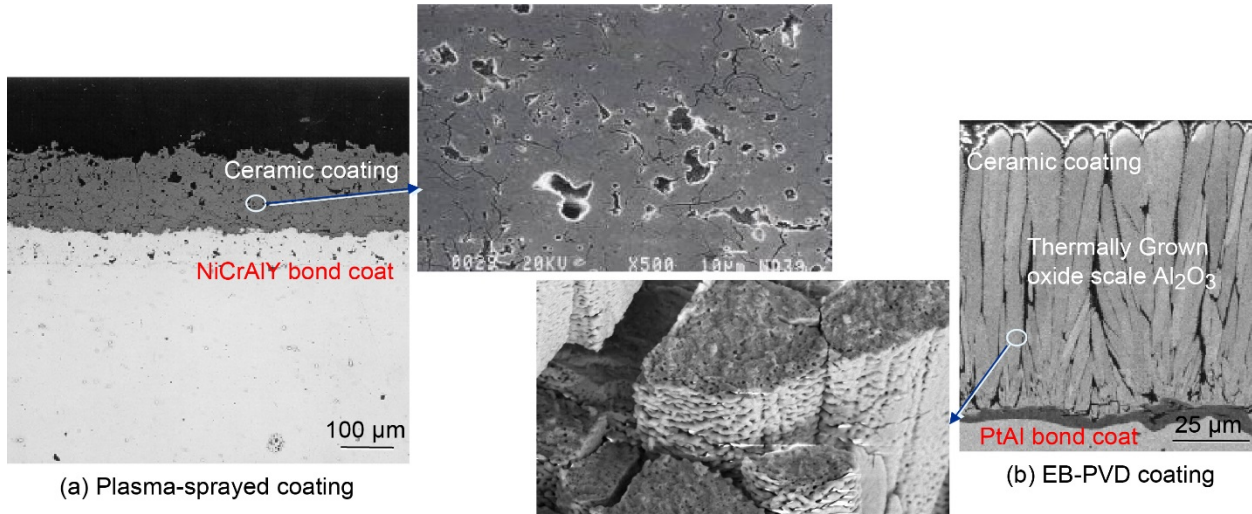


Figure 2.—Microstructures of thermal barrier coatings (TBCs) on metallic substrates. (a) A plasma-sprayed TBC system; (b) an electron beam-physical vapor deposition (EB-PVD) TBC system.

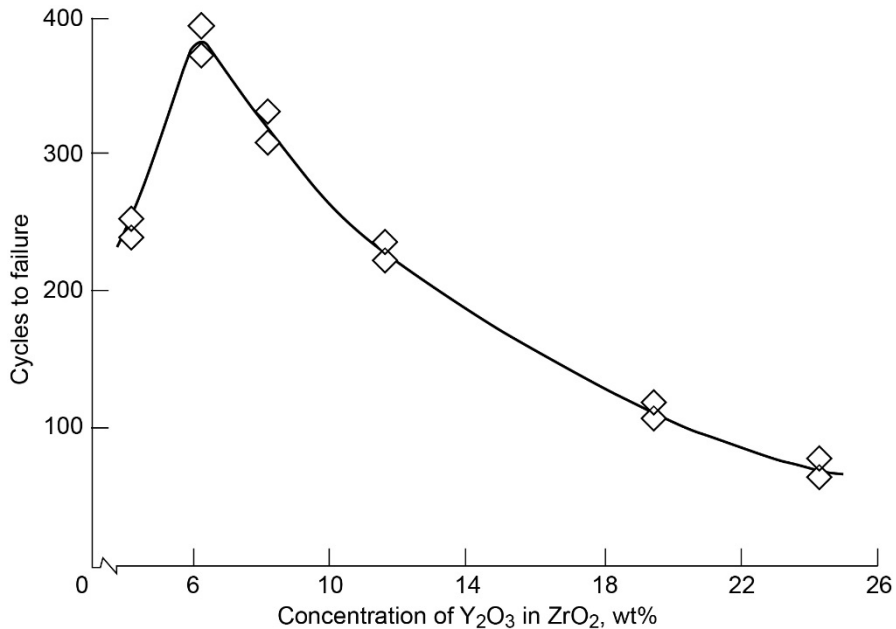


Figure 3.—NASA's early studies show the best furnace cyclic life and durability for the thermal barrier coating (TBC) systems with a composition of  $ZrO_2 - 6 \text{ to } 8 \text{ wt\% } Y_2O_3$  (Ref. 15).

Although  $t'$  phase coatings have the advantages of higher toughness and are generally more durable for rotating components, where erosion and impact resistance can be of major concern, the coating materials intrinsically are metastable, and therefore their use temperature is limited to 1200 to 1250 °C for long-term operation in turbine engine environments. The  $t'$  coatings also have higher thermal conductivity and fast sintering (ceramic coating densification) that can reduce the coating initial porosity, resulting in the significant thermal conductivity increase and reduced cyclic durability (Refs. 17 and 18). To further increase the turbine engine efficiency and operating temperatures, higher temperature and lower thermal conductivity coating systems have been in development in last two decades (Refs. 19 to 23). Among the advanced low thermal conductivity thermal barrier coatings are the multicomponent defect-clustering coatings (Ref. 23). The advanced oxide coatings were designed by incorporating multicomponent, paired-cluster dopants in conventional zirconia-yttria oxides. The dopant oxides were selected based on the cation-anion interatomic and chemical potentials, lattice elastic strain energy, polarization and the electro-neutrality of the oxides. Because defect clusters can attenuate and scatter lattice phonon waves as well as radiative photon waves at a wide spectrum of frequencies, the coatings have significant reductions in the oxide intrinsic lattice and radiation thermal conductivity. The creation of the thermodynamically stable and highly distorted lattice structures, with essentially immobile defect clusters and/or nanoscale ordered phases, effectively reduces the mobile defect concentration and suppress the atomic mobility and mass transport, thus significantly improving the oxide sintering-creep resistance and mechanical properties. Thermal conductivity of various multicomponent defect cluster thermal barrier coatings, along with other advanced low thermal conductivity thermal barrier coatings, are summarized in Figure 4(a) to (c), (Refs. 23, 24, and 9). These figures show thermal conductivity of various multicomponent defect cluster and other types of advanced low thermal conductivity thermal barrier coatings, as function of dopant concentrations, and compared with the  $t'$  phase  $ZrO_2$ -(6-8) wt%  $Y_2O_3$ . The sintering-induced thermal conductivity increases are also shown as the coating thermal conductivity values for as-processed ( $k_0$ ), after 5 and 20 hr at temperatures ( $k_5$  and  $k_{20}$ ). The advanced defect cluster thermal barrier coatings showed lower initial thermal conductivity (as-processed thermal conductivity  $k_0$ ), as well as slower increases in the sintering induced thermal conductivity, as characterized from the conductivity values of the coatings after 5 and 20 hr at temperatures ( $k_5$  and  $k_{20}$ ). A low thermal conductivity defect cluster coating,  $ZrO_2$ -9.5wt%  $Y_2O_3$ - 5.6 $Yb_2O_3$ -5.2 $Gd_2O_3$ , rare earth zirconate ( $Gd_2Zr_2O_7$  and  $Sm_2Zr_2O_7$ ), and a few other compositions and their specifications may be found in the literature (Refs. 25, 26, 12, and 27).

Figure 4(a) to (c): (a) Plasma spray low conductivity defect cluster coatings; (b) EB-PVD defect cluster coatings; (c) Thermal barrier coating with various dopant concentrations. These figures show thermal conductivity of various multicomponent defect cluster and other types of advanced low thermal conductivity thermal barrier coatings, as function of dopant concentrations. The data are compared with the  $t'$  phase  $ZrO_2$ -(6 to 8) wt%  $Y_2O_3$ . The sintering induced thermal conductivity increases are also shown as the coating thermal conductivity values for as processed ( $k_0$ ), after 5 and 20 hr at temperatures ( $k_5$  and  $k_{20}$ ).

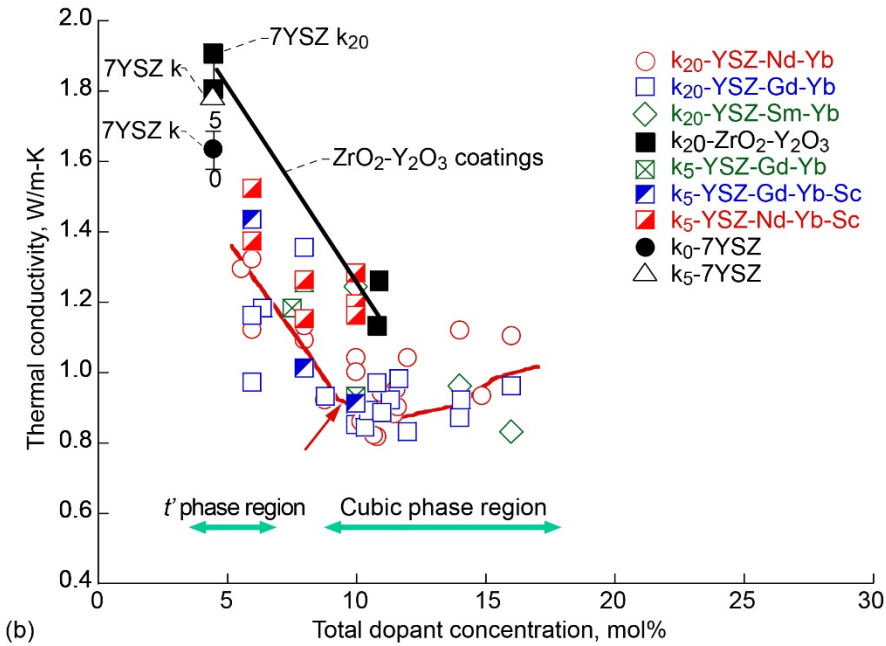
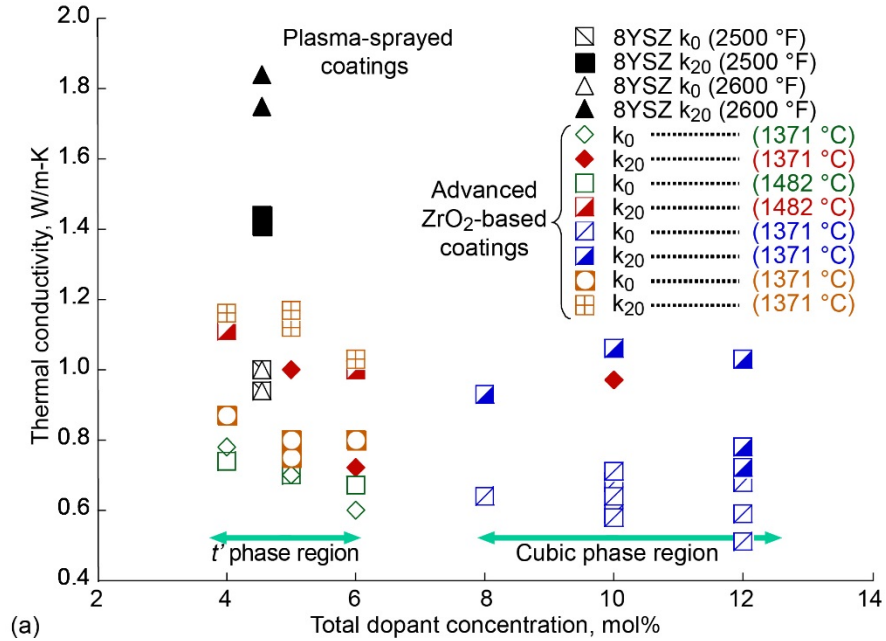


Figure 4.—(a) Plasma-sprayed thermal barrier coatings (TBCs), thermal conductivity tested 1371 and 1482 °C (Ref. 24). (b) EB-PVD TBCs, thermal conductivity tested 1316 °C (Refs. 23 and 9). (c) Thermal conductivity comparisons for various advanced composition EB-PVD thermal barrier coatings, including YSZ, multicomponent defect cluster coatings, and  $Gd_2Zr_2O_7$  (Ref. 9).

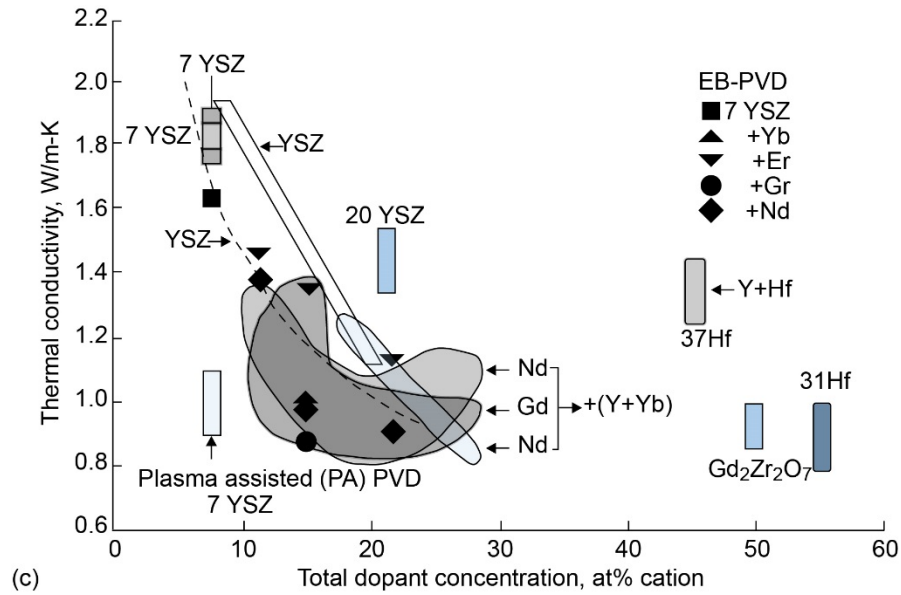
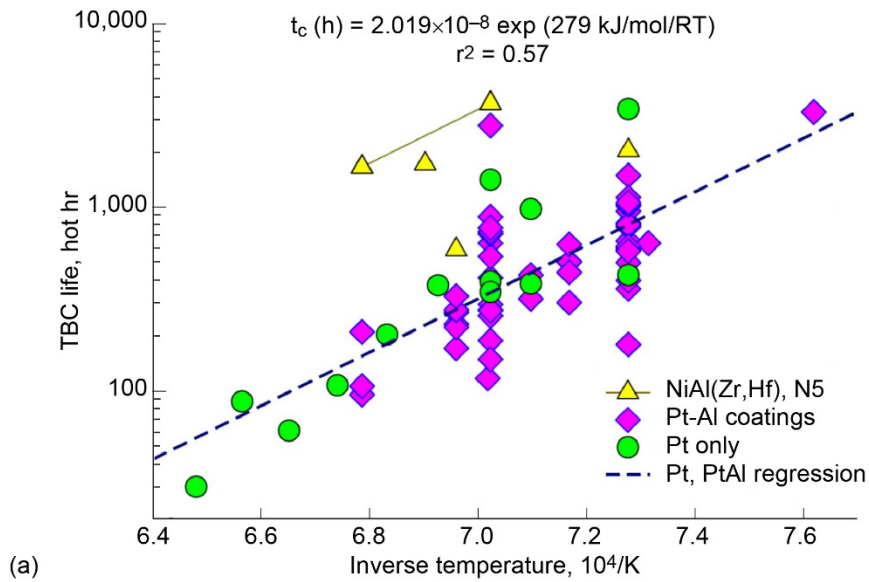
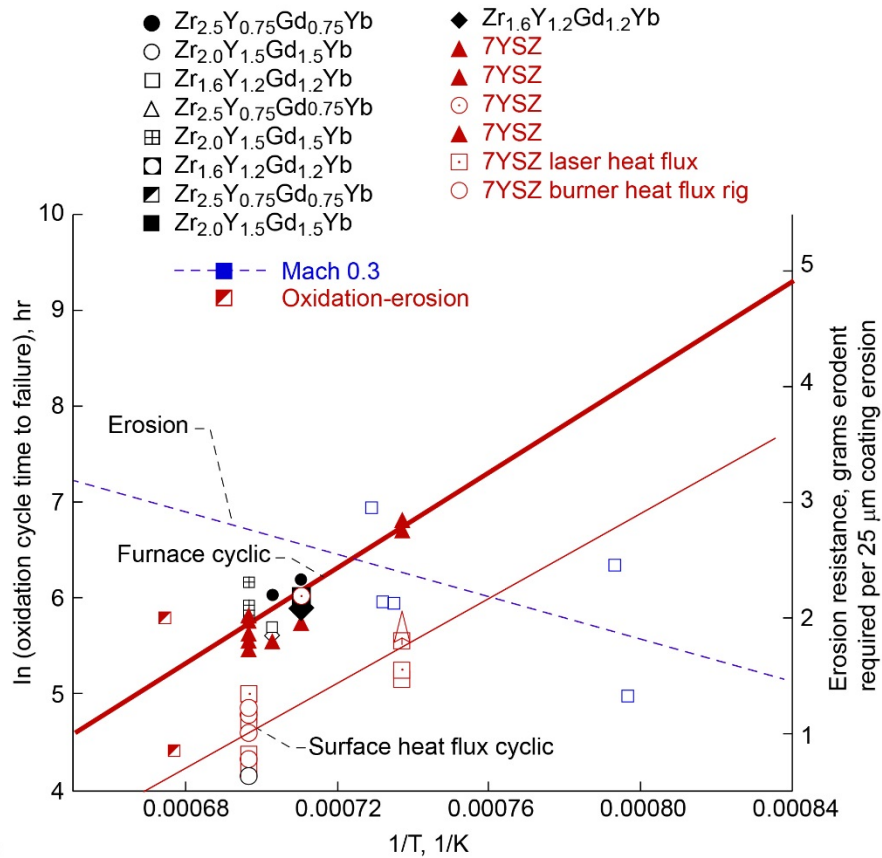


Figure 4.—Concluded.

Future TBC systems will be more aggressively designed for the thermal protection of engine hot-section components, thus allowing significant increase in engine operating temperatures, fuel efficiency and engine reliability. However, the coating reliability and durability under high temperature, high thermal gradient cyclic conditions still remain as major challenges (Refs. 18, 28, and 29). Particulate erosion, impact, and engine ingested low melting calcium magnesium aluminosilicate sand dusts or volcanic ashes during service have further complicated the life designs of turbine airfoil TBCs (Refs. 30 to 35). Figure 5(a) and (b) shows cyclic lives of turbine airfoil thermal barrier coatings under various temperature conditions and degradation mechanisms. The coating life is exponentially reduced with increasing temperature, because interface damage effects are significantly increased from the accelerated oxide scale growth and increased cyclic stress-temperature amplitudes during the cycling, as shown as Arrhenius behavior of furnace cyclic lives. The erosion – bond coat oxidation based failure map for 7YSZ and defect cluster low conductivity thermal barrier coatings, also showing the Mach 0.3 particulate erosion is a more dominated failure mode at lower temperatures while the surface heat flux can reduce thermal barrier coating cyclic life and durability. The erosion-based coating failure life can be increased with temperature because the  $t'$  phased coating toughness and plasticity increase with temperature (Ref. 32). The coating failure modes are usually complex, largely depending on envisioned engine operating conditions, processed coating composition, architecture and microstructures. The increases in engine temperature, pressure and heat flux can raise durability issues for current coating systems. The development of next generation advanced thermal barrier coatings will greatly rely on better understanding of the coating behavior and failure modes under the high-temperature, high-thermal gradient cyclic conditions.



(a)



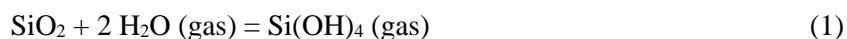
(b)

Figure 5.—(a) Arrhenius behavior of furnace cyclic lives of EB-PVD thermal barrier coatings (TBCs) compiled for 7YSZ TBCs using NiAl and Pt Al bond coats (Ref. 29). (b) The erosion – bond coat oxidation based failure map for 7YSZ and defect cluster low conductivity TBCs, showing the Mach 0.3 particulate erosion is a more dominated failure mode at lower temperatures while the surface heat flux can reduce TBC cyclic life and durability (Ref. 32).

## Environmental Barrier Coatings (EBCs)

The ever-increasing demands for developing more efficient, low emission and high performance aircraft and space vehicle propulsion engines have required new hot-section component materials that are significantly lighter and with higher temperature capabilities. Current nickel-based superalloys are reaching the upper limit of their temperature capabilities, and therefore SiC fiber-reinforced SiC/SiC ceramic matrix composites (CMCs) have been envisioned as alternative next generation turbine engine hot-section materials (Refs. 7, 36, 37, and 8). Silicon-based ceramics and composites, such as SiC/SiC ceramic matrix composites, are desirable because they have low density, high temperature creep strength and oxidation resistance in dry oxidizing environments. Environmental barrier coatings (EBCs) are required to prevent the SiC/SiC CMCs from water vapor attack in engine combustion environments, due to volatilization of the protective silica (SiO<sub>2</sub>) scales on SiC when reacting with water vapor during the operation (Ref. 38). The loss of SiO<sub>2</sub> from the ceramic surfaces leads to the accelerated strength degradation under combined thermal and mechanical loading conditions in the engine operating environments. Therefore, environmental barrier coatings are considered essential in enabling the CMC component technologies for next generation aerospace propulsion engine systems.

The SiO<sub>2</sub> surface recession occurs when the SiO<sub>2</sub> scale reacts with water vapor in engine combustion environments, forming gaseous Si(OH)<sub>4</sub> and thus resulting in the volatilization of the SiO<sub>2</sub> scales of SiC/SiC CMC materials (Ref. 38). The volatilization and reaction occurs with the water vapor according to the following equation:



The surface recession mechanism is dependent on the gas velocity and can be dramatically accelerated as the velocity increases (Refs. 38 and 39). For turbine engine conditions, the velocity factor is related to the gas Mach number and/or heat transfer coefficient, and film-cooling can also be integrated, studied and modeled (Ref. 40). Figure 6 depicts a schematic diagram of the SiC/SiC CMC recession due to SiO<sub>2</sub> volatility in a convective and convective plus film cooling conditions (Ref. 40). For the SiC forming SiO<sub>2</sub> scale with the unit silica activity, the surface recession rate  $K_{\text{recession}}$ , due to the silica volatilization by the reaction with water vapor has the velocity and pressure dependence according to Equation (2) (Ref. 38):

$$K_{\text{recession}} = C V^{1/2} P_{(\text{H}_2\text{O})}^2 / (P_{\text{total}})^{1/2} \quad (2)$$

where

$C$  constant  
 $V$  gas velocity  
 $P_{(\text{H}_2\text{O})}$  total partial pressure of water vapor  
 $P_{\text{total}}$  total combustion chamber pressure

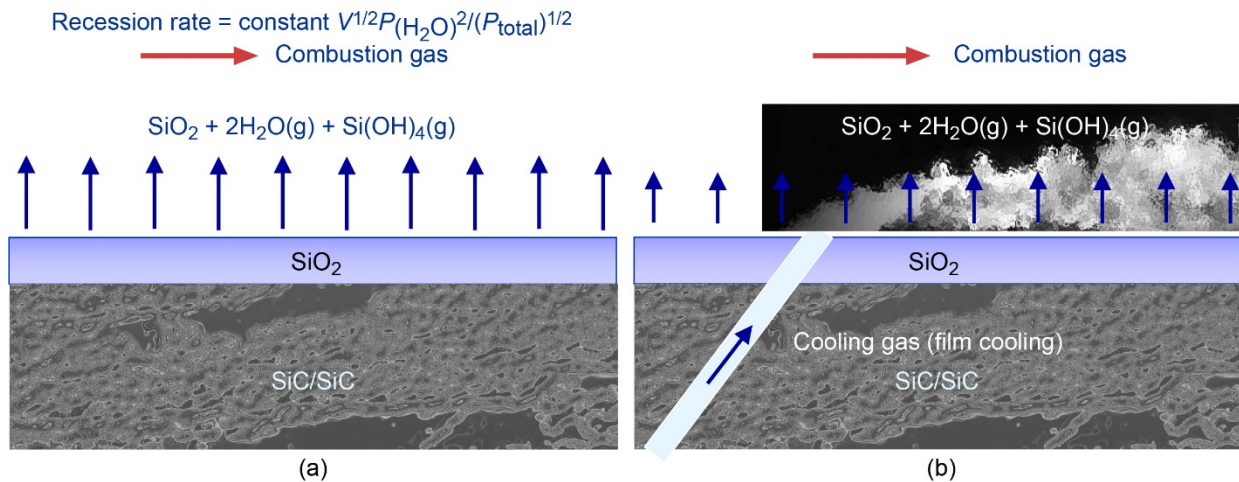


Figure 6.—Schematic diagram showing the surface recession of SiO<sub>2</sub> scales on a SiC/SiC ceramic matrix composite specimen. (a) Recession in a convective combustion gas flow. (b) Recession in a convective combustion gas and film-cooling air flow. In a film cooling case, more complex analysis including Computational Fluid Dynamics (CFD) analysis are needed to understand the local gas flow velocity, pressure and water vapor fractions (Ref. 40).

The early generation EBCs consist of Si bond coat, mullite-based intermediate coat and barium-strontium-aluminosilicate (BSAS, Ba<sub>1-x</sub>Sr<sub>x</sub>Al<sub>2</sub>Si<sub>2</sub>O<sub>8</sub>; 0 < x < 1) top coat, developed in the NASA Enabling Propulsion Materials (EPM) Program (Refs. 41, 42, 12, and 43). The EBC material systems have shown a good compatibility with SiC/SiC CMC systems, and the coating feasibility and durability have also been tested in various land based turbine validation tests (Refs. 44 to 46). The temperature limits and stability of the first generation environmental barrier coating systems have also been well studied, the use temperature is generally limited to 1300 °C in contact with the silicon bond coats (Refs. 47 to 49). As an example, for BSAS, Ba<sub>1-x</sub>Sr<sub>x</sub>Al<sub>2</sub>Si<sub>2</sub>O<sub>8</sub>; 0 < x < 1 environmental barrier coating case, the surface recession rate in micrometer per hour, is determined by the following equation (Refs. 46 and 7)

$$K_{\text{recession}}(\text{BSAS}) = 10^{-5654/[T^{\circ}\text{C}+273]} x P^{1.5} x V^{0.5} x a_{\text{SiO}_2} \quad (3)$$

where  $a_{\text{SiO}_2}$  = the SiO<sub>2</sub> activity in the EBC. The lower activity of BSAS resulted in a reduced recession rate of the EBC coated SiC/SiC CMC systems.

The next generation engine systems currently envisioned with higher component operating temperatures demand more advanced environmental barrier coating systems. The second-generation EBCs have temperature capability up to 1482 °C, using rare earth metal or transition metal disilicate and monosilicate compositions with low silica activity (e.g., Yb<sub>2</sub>Si<sub>2</sub>O<sub>7</sub>, Gd<sub>2</sub>Si<sub>2</sub>O<sub>7</sub>, Er<sub>2</sub>Si<sub>2</sub>O<sub>7</sub>, Y<sub>2</sub>SiO<sub>5</sub>, Yb<sub>2</sub>SiO<sub>5</sub>, Gd<sub>2</sub>SiO<sub>5</sub>), for protecting SiC/SiC ceramic matrix composites (Ref. 50). Recent laboratory mass spectrometric measurements showed that the rare earth silicates have low silica activities, thus possessing low volatility (Ref. 51). Third-generation coatings include advanced thermal and environmental barrier coating systems with surface temperature capability up to 1650 °C (Refs. 7 and 52). Some recession rates for selected environmental barrier coatings including BSAS are shown in Figure 7, and compared with the SiC/SiC CMCs and Si<sub>3</sub>N<sub>4</sub> monolithic ceramics. The recession rates are determined using NASA's High Pressure Burner Rig in conditions of up to 16 atm, and 200 m/s combustion gas velocity, at various temperatures. The SiO<sub>2</sub> recession rates on SiC/SiC CMC have also been determined at 1300 °C, as shown in Figure 8, with the approximate gas velocity dependence of 0.46 to 0.6, and total pressure dependence of 1.97 (at water vapor partial pressure approximately 9 percent) (Ref. 40).

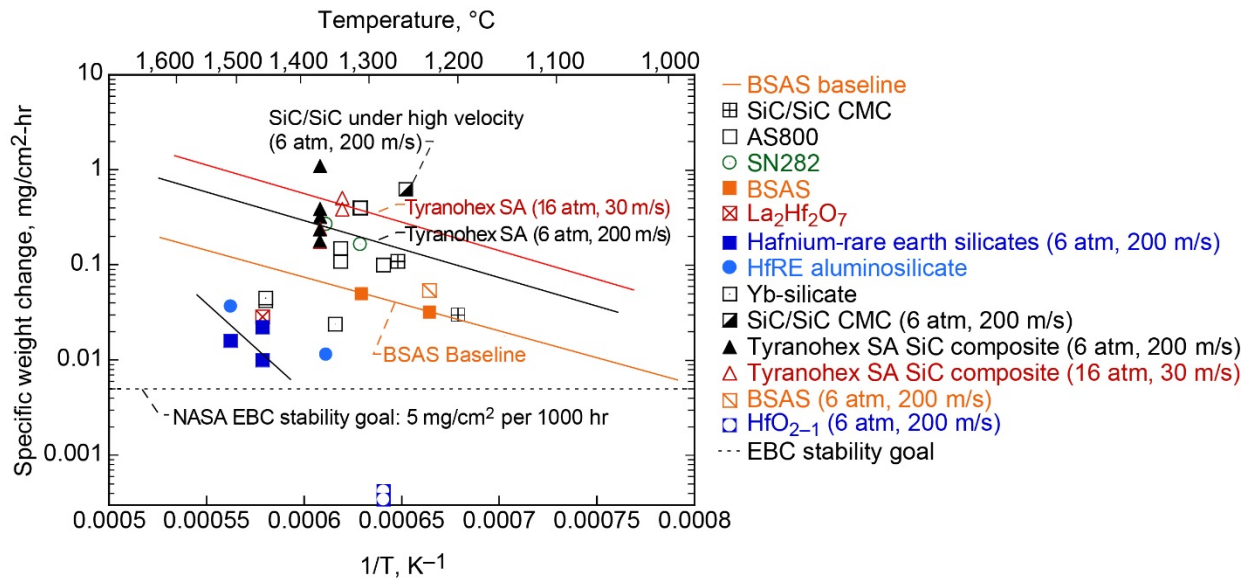


Figure 7.—Environmental barrier coating (EBC) recession determined under high pressure and high gas velocity conditions (Ref. 40). The test pressure was generally at 6 atm with the gas velocity of 30 m/s unless otherwise indicated.

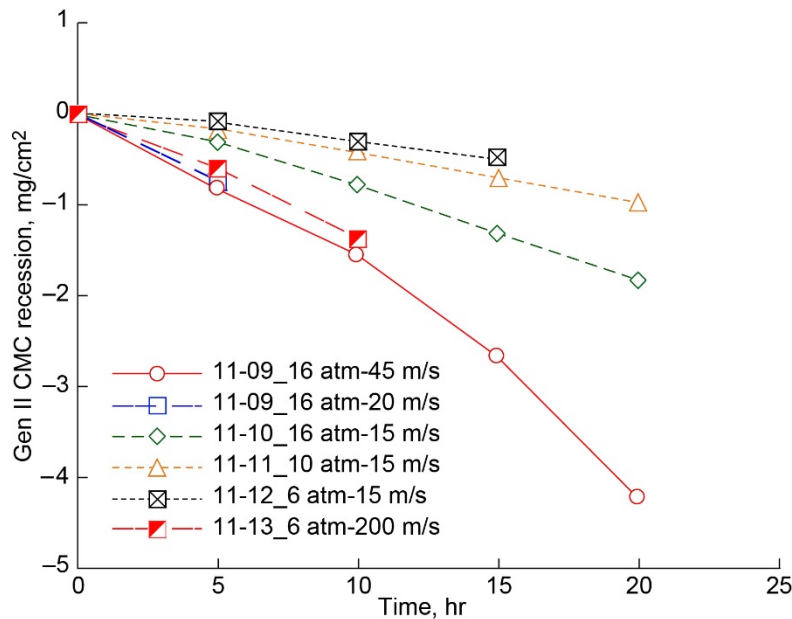


Figure 8.—The SiC/SiC recession rates at 1300 °C under various pressure and gas velocity conditions (Ref. 40).

Multicomponent rare earth–silicates, hafnium–aluminosilicates, and hafnium - rare earth silicate EBC systems, along with hafnia ( $\text{HfO}_2$ )–silicon, and rare earth–silicon based bond coat systems have also recently been used for 1500 °C capable EBC systems to significantly improved temperature capability and calcium magnesium aluminosilicate (CMAS) resistance (Refs. 43, and 53 to 56). Table I illustrates the advanced environmental barrier coating materials and multilayer structures that have evolved for improving temperature capability, environmental stability, and toughness for turbine engine applications. The EBCs have evolved from BSAS to rare earth silicates to rare earth – hafnium – silicate multicomponent

TABLE I.—EVOLUTION OF NASA EBC TECHNOLOGY FOR SiC/SiC CERAMIC MATRIX COMPOSITES: EBC SYSTEM DEVELOPMENTS

EBC configurations	Gen I 1995 to 2000 R&D Award	Gen II 2000 to 2004	Gen III 2000 to 2005 US 7,740,960 B1	Gen IV 2005 to 2011 R&D Award (2007) Turbine airfoil EBS development US 7,740,960 B1	Gen V 2007 to 2012	Gen VI 2009 to present Patent S/N: 13/923,450; PCT/US 13/46946; 15/582,874; 15/625,277; 15/13,821; 15/824,036; 15/882,435
Engine components	Combustor	Combustor/ (vane)	Combustor/vane (hybrid plasma spray EB-PVD processing)	Turbine vane/ turbine blade	- Vane/blade EBCs - Equivalent APS combustor EBCs	Airfoil components
Top coat	BSAS (APS)	RE <sub>2</sub> Si <sub>2</sub> O <sub>7</sub> or RE <sub>2</sub> SiO <sub>7</sub> (APS)	- (Hf,Yb,Gd,Y) <sub>2</sub> O <sub>3</sub> - ZrO <sub>2</sub> /HfO <sub>2</sub> – RE silicates - ZrO <sub>2</sub> /HfO <sub>2</sub> + BSAS (APS and EB-PVD)	RE-HfO <sub>2</sub> -alumino silicate  (APS and EB-PVD)	RE-Hf-silicate; RE-HfO <sub>2</sub> -graded silica processing (EB-PVD)	Advanced RE-Hf+X silicates
Interlayer	-----	-----	RE-HfO <sub>2</sub> /ZrO <sub>2</sub> - aluminosilicate layered systems	Nanocomposite graded oxide/silicate	Gen IV interlayer not required (optional)	-----
EBC	Mullite+BSAS	BSAS + mullite	RE silicates or RE-Hf silicates	RE dope mullite- HfO <sub>2</sub> or RE silicates	Multicomponent RE silicate systems	Multicomponent RE silicate/self-grown
Bond coat	Si	Si	Oxide+Si bond coat	HfO <sub>2</sub> -Si-X, doped mullite/Si SiC nanotube	Optimized Gen IV HfO <sub>2</sub> -Si-X bond coat 1482 °C bond coat	RE-Si+X based systems
Thickness	250 to 400 μm	250 to 400 μm	250 to 500 μm	250 μm	127 μm	25 to 100 μm
Surface temperature capability	Up to 1316 °C	1316 °C	1650 °C with 1316 °C CMC	1482 °C with 1316 °C CMC	Up to 1650 °C with 1316 °C, 1482 °C CMC	Up to 1650 °C with 1316 °C, 1482 °C CMC
Bond coat temperature capability	Limited to 1350 °F	Limited to 1350 °F	Limited to 1350 °F	1420 °C+; advancement 1482 °C	1482 °C (2011 goal)	1482 °C+ (TRL 3 to 5)

Notes: “X” indicates alloyed dopants.

EBCs, while the EBC bond coats have also advanced from silicon to hafnia (HfO<sub>2</sub>) – silicon, rare earth – silicon to rare earth - hafnium – silicon systems with controlled oxygen and silicon activities for ceramic matrix composite turbine airfoil applications (Ref. 57). The rare earth silicate–mullite or alumina coating systems have also been recently considered beneficial because of significantly lower oxygen permeability for mullite and Al<sub>2</sub>O<sub>3</sub> as compared with that for the ytterbium disilicate EBC (Refs. 58 and 59). Low diffusion and Ultra-High Temperature Ceramic (UHTC) protective coatings or composites are also being developed (Refs. 60 to 62).

The design of environmental barrier coatings for aerospace propulsion engines have significantly benefited from early generation monolithic coating developments, and also from the turbine thermal barrier coating experience. In general, coating material system design considerations should include coating temperature capability, environmental and mechanical stability, chemical compatibility (e.g., no reactions occurring forming low melting phases), and phase stability during the service operation. High toughness and low thermal conductivity are important properties for turbine airfoil environmental barrier coatings, where a thin coating is required for aerodynamic requirements, ensuring durability in high-pressure and high-velocity gas flow, and for particulates or molten sand impingements during service. As shown in Figure 9, coatings should be designed to be operated in a safe region (shadow area) where lower

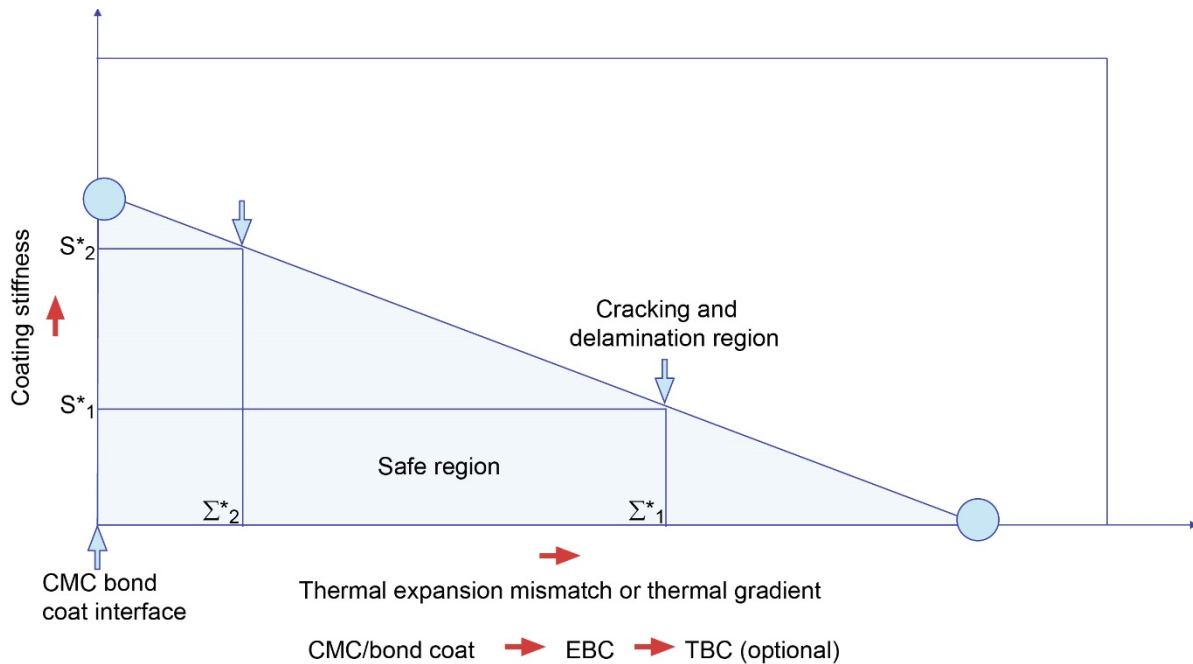


Figure 9.—The environmental barrier coating (EBC) mechanical stability safe design approach: with increasing distance from the bond coat towards surface EBC layers, the coating system generally has increased thermal expansion mismatch stresses or thermal gradients (due to lower thermal conductivity of the top coatings), thus the stiffness should be reduced to ensure higher strain tolerance and to maintain the coating stability and durability.

stiffness coatings should be designed to increase the strain tolerance when higher thermal stresses from a larger thermal expansion mismatch or large thermal gradient is present. With increasing distance from the bond coat toward surface EBC layers, the coating system generally has increased thermal expansion mismatch stresses or thermal gradients (due to lower thermal conductivity of the top coatings). Thus the stiffness should be reduced to ensure higher strain tolerance and to maintain the coating stability and durability.

The EBCs have demonstrated the feasibility and significantly improved high temperature and environmental stability of the EBC-CMC systems in laboratory testing and simulated engine rig conditions (Refs. 43, 63, and 64), and SiC/SiC CMC turbine shrouds have been incorporated in the engine design and applications. Challenges still remain for significantly improved environmental durability and thermomechanical fatigue resistance in turbine engine high heat flux environments to achieve the prime-reliant environmental barrier coating designs in aero turbine environments.

### SiC/SiC Ceramic Matrix Composites (CMCs)

SiC/SiC ceramic matrix composites reinforced by continuous-length, polycrystalline high strength SiC fibers are revolutionary hot-section materials for aerospace propulsion engines. Significant progress has been made in the development and recent implementation of SiC/SiC ceramic matrix composite materials for the engine hot section components (Refs. 37 and 7). The engine performance benefits are attributed to the low density, higher temperature capability, and resistance to oxidation and corrosion of SiC/SiC composites, thereby allowing designs with higher component temperature and reduced cooling as compared to nickel base superalloys. The weight reductions realized by applying SiC/SiC CMC to engine rotating components can further reduce the design complexity and weight of engine structures. The

temperature capability of the current-state-of-the-art SiC/SiC CMC systems have the temperature capability of 1316 °C (2400 °F), which is an improvement with a potential temperature benefit over superalloys exceeding 200 °C. As shown in Figure 10, the development of enabling CMC and environmental barrier coatings, will result in a step increase in the temperature capability of gas turbine components. Generation II CMCs have a temperature capability of 1316 °C, which is an improvement, whereas future generation CMC materials are envisioned to be capable of 1482 °C when advanced SiC fibers and matrix materials are used.

The SiC/SiC CMCs generally have two processing routes. The first route was developed and demonstrated in the NASA Enabling Propulsion Material (EPM) Program under a CMC combustor program (Refs. 65 and 37). The method emphasizes chemical vapor infiltration (CVI), by first applying a CVI-BN fiber interphase coating (0.1 to 0.5 μm thickness) for the SiC fiber tow preform, followed by a thin matrix CVI-SiC layer over the BN interphase coating. This CVI process is then followed by a SiC fine particulate slurry infiltration at room temperature, and finally ends with a silicon melt Infiltration (MI) at 1400 °C. This process is often referred to as the CVI-SMI or CVI-MI process and is illustrated in Figure 11(a).

The second CMC process route was developed by General Electric for processing SiC/SiC (HiPerComp) turbine engine components (Ref. 66). This method fabricates prepregged unidirectional 2D tapes, by using a polymer-based binder containing SiC, Si and carbon particulates, along with CVI processing precoated fiber tows. The 2-D tapes can be stacked into 3-D preforms, heated to high temperature (1400 to 1450 °C) for casting and melt-infiltration of CMC components by a reactive melt-infiltration process. The HiPerComp SiC/SiC CMCs have residual silicon levels of 5 to 15 vol% and also generally requires thicker fiber coatings (1 μm, typically BN, Si-doped BN, SiC and Si<sub>3</sub>N<sub>4</sub>) to prevent the fibers to be reacted with silicon at the high-temperature reactive process. The detailed HiPerComp CMC thermophysical, elastic and fracture strength properties are given in the Reference 44. Figure 11(b) illustrates the prepreg – melt-infiltration processes for SiC/SiC ceramic matrix composites.

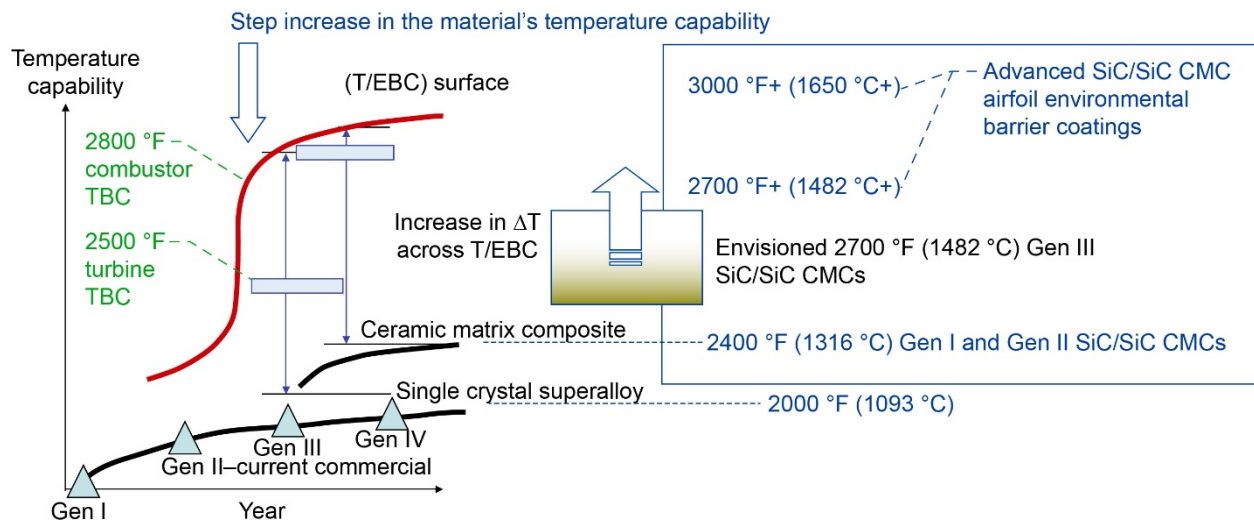


Figure 10.—The development and implementation of SiC/SiC CMC along with advanced ceramic environmental barrier coatings will result in a step increase in the temperature capability of gas turbine hot-section components. The Generation II CMCs have the temperature capability of 1316 °C, which is an improvement while the future generation CMC materials are envisioned to be capable of 1482 °C when advanced SiC fibers and matrix materials are used.

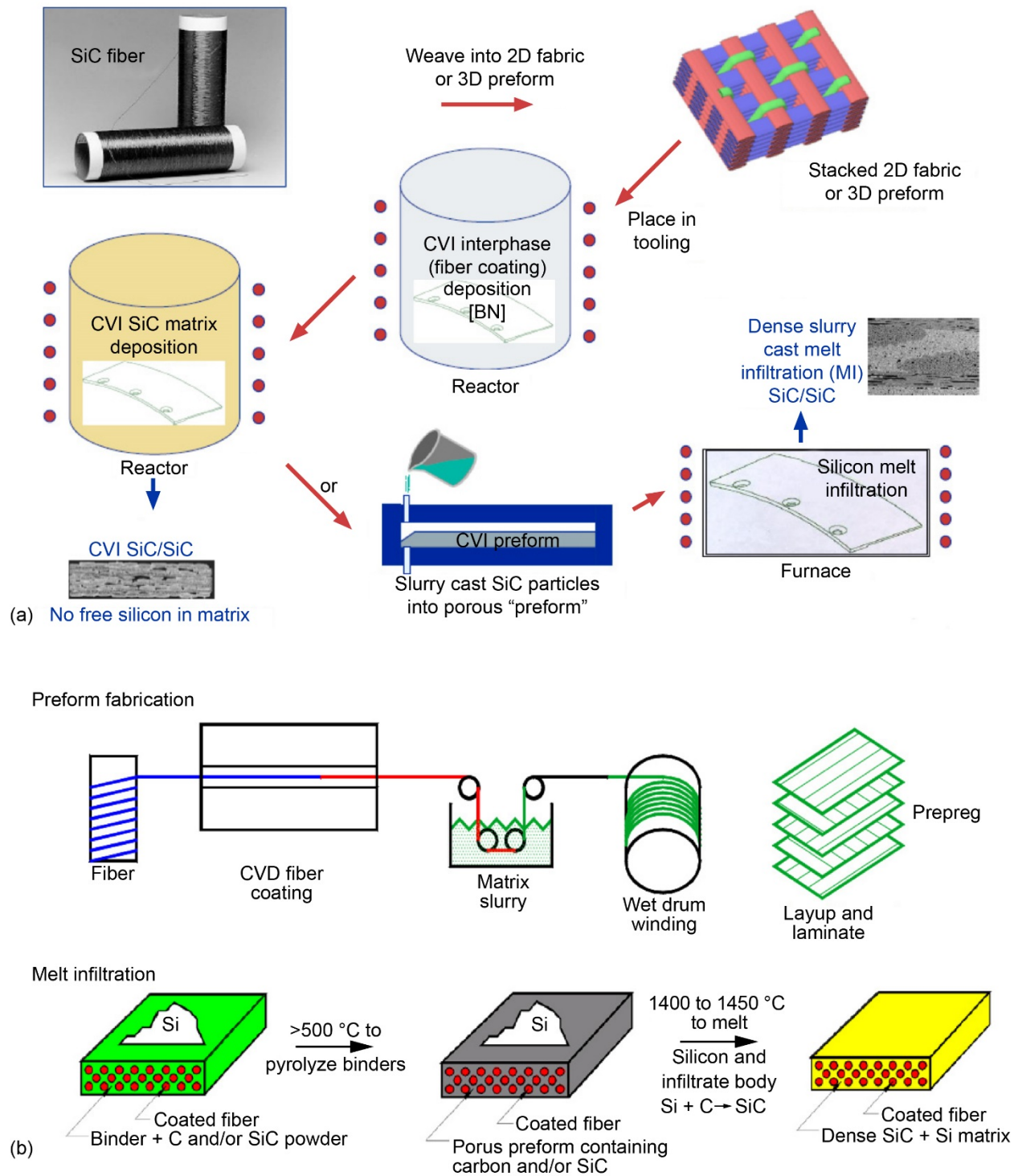


Figure 11.—Two representative SiC/SiC ceramic matrix composite processing routes. (a) NASA EPM CVI-SMI CMC process (Ref. 65); (b) General Electric Prepreg, Melt Infiltration CMC process (Ref. 67).

Advances have been made in the various materials constituents of CMCs. Ceramic fibers, in particular, play a significant role in the high performance CMCs. Factors affecting the SiC fiber creep and rupture properties include grain size; impurities, such as the residual oxygen content (in particular

affecting the primary creep stage, grain boundary relaxation), porosity and surface roughness and other defects. The steady-state creep strain rate  $\dot{\epsilon}$  (percent strain per hour) of the ceramic fibers can be written as (Refs. 37 and 68)

$$\dot{\epsilon}_{\text{steady-state}} = (C/d) \sigma^n \exp(-Q_s/RT) \quad (4)$$

where

- $C$  an empirical constant
- $d$  average grain size, nm
- $\sigma$  applied stress, MPa
- $n$  stress exponent
- $Q_s$  secondary or steady-state creep activation energy
- $R$  gas constant
- $T$  temperature in kelvin

Table II summarizes the key fiber process and creep-related properties for two important fiber types, Hi-Nicalon-Type S and Sylramic-iBN SiC fibers. Figure 12 shows the creep-stress rupture curves for selected materials. Hi-Nicalon-Type S and Sylramic-iBN fiber reinforced composites have good rupture life at the envisioned 1315 °C (Refs. 68 and 37).

TABLE II.—HIGH TEMPERATURE SiC/SiC CMM SiC-BASED FIBER CREEP PROPERTIES

Fiber types	Maximum use temperature, °C	Elastic modulus E, GPa	Tensile strength, GPa	Creep constant, C	Stress exponent, n	Grain size, nm	$Q_s$ , kJ/mole
Hi-Nicalon-Type S (Nippon Carbon)	1650	355	2.6 to 2.8	$2.2 \times 10^{16}$	3	20	814
Sylramic-iBN (NASA)	1800	380	3.1	$7.0 \times 10^{17}$	3	250	814

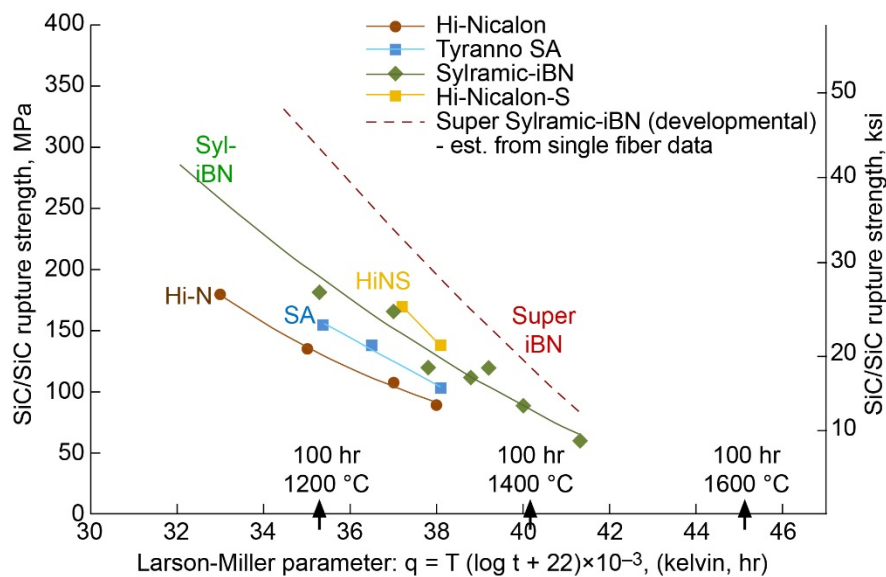


Figure 12.—The Larson-Miller plot for CVI-SMI SiC/SiC ceramic matrix composites with various fiber types as 2-D 0/90-balanced fabric with approximately 18 percent fiber volume fraction aligned in stress direction (Refs. 68 and 37). Hi-Nicalon-Type S and Sylramic-iBN fiber reinforced composites have good rupture life at the envisioned 1315 °C.

CMC development has been continuing for achieving 1482 °C+ temperature capabilities (Ref. 69). The polycrystalline fiber development efforts focused on thermal–chemical treatments to increase fiber grain size and grain size uniformity, reduce porosity and defects by sintering, and reduce and modify the grain boundary low-viscosity phases. Advanced CMC architectures for achieving higher fiber volume fractions, 3-D fiber architectures and CVI for improved rupture and interlaminar strengths have also been in development (Refs. 37 and 70). Some examples of 3-D architecture CMCs are shown in Figure 13. Hybrid CMC processing by chemical vapor infiltration – polymer-infiltration and Pyrolysis (CVI-PIP), with multiple PIP cycles, has achieved silicon-free, dense matrix, and have shown improved temperature capability and rupture to 1482 °C. It looks promising with improved through thickness thermal conductivity (Refs. 37 and 71). Figure 14 shows an example of high heat flux, thermal gradient testing results of advanced EBC coated CVI+SMI (average CMC and hybrid CVI-PIP CMCs), demonstrating 300 to 400 hr creep and fatigue durability at 2700 °F (1482 °C) (Ref. 72). The advanced CVI-PIP CMC material showed low creep strains at significantly higher temperatures as compared with the CVI-SMI CMCs. The high heat flux simulated engine environment fatigue life durability of environmental barrier coated prepreg melt infiltration (MI), CVI-SMI, and CVI-PIP SiC/SiC CMC systems has also been highlighted in the literature (Refs. 43, 64, and 60).

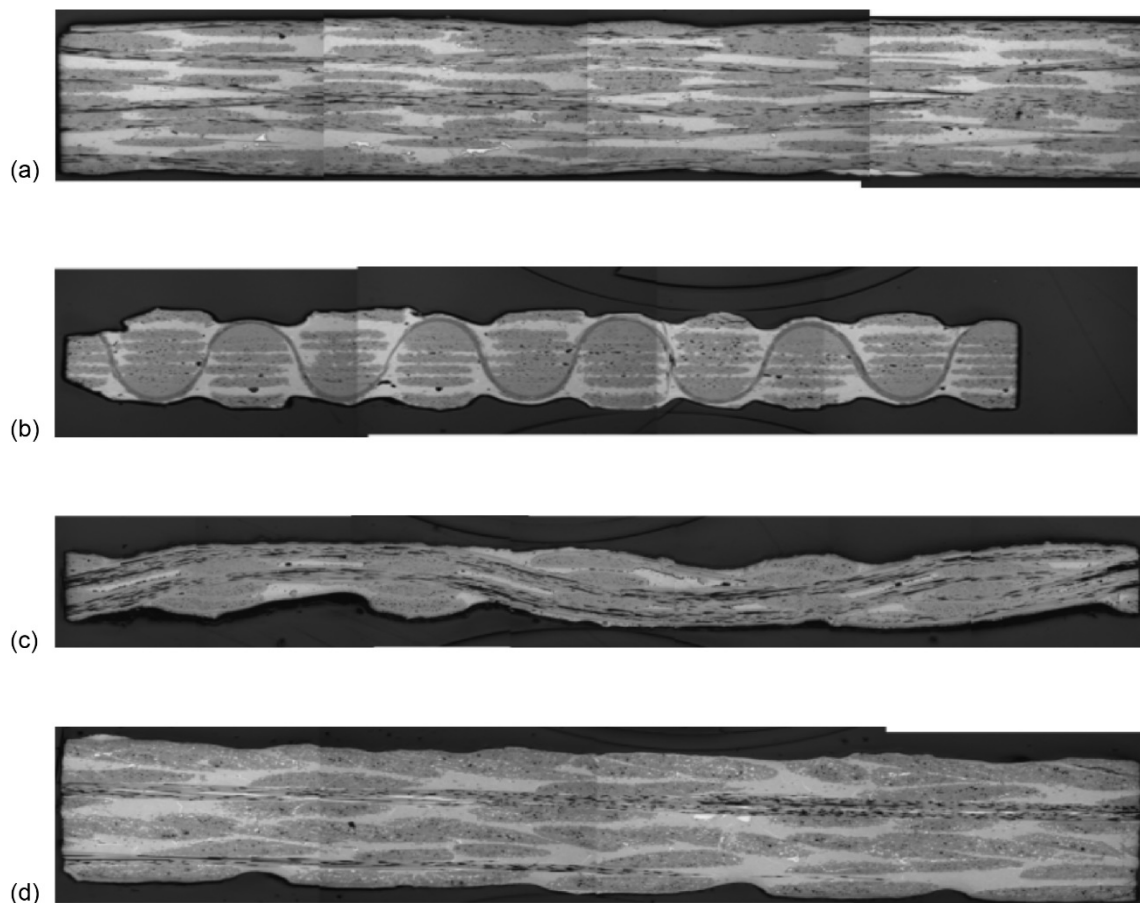


Figure 13.—Various SiC/SiC CMC architecture designs for improved rupture and interlaminar strengths (Refs. 73 and 70). (a) 2-D five-harness satin. (b) 3-D orthogonal. (c) Angle interlock. (d) Braid.

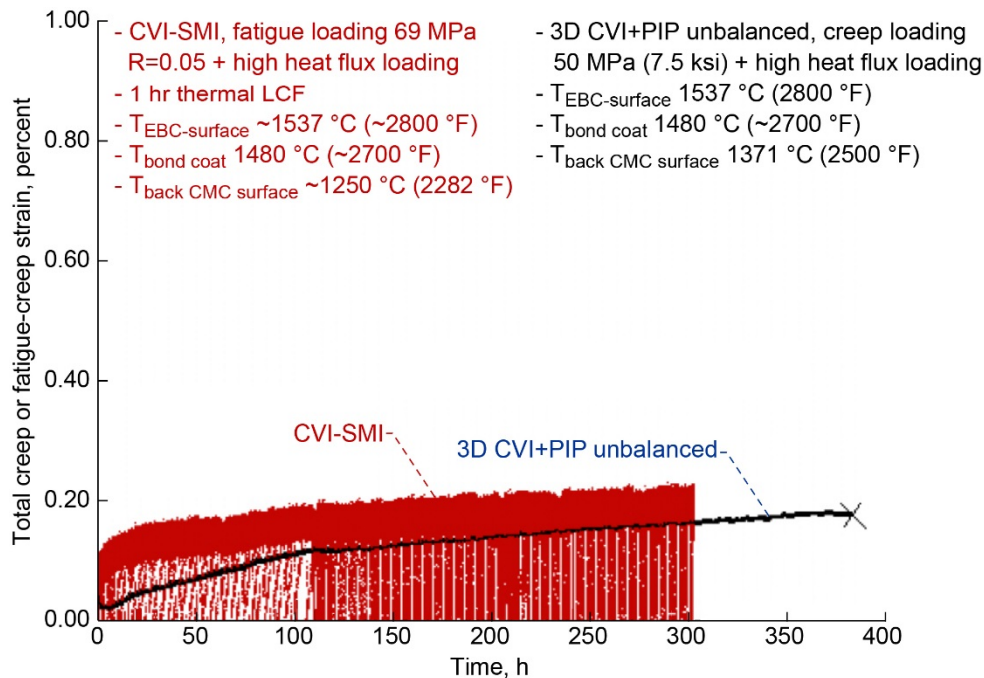


Figure 14.—Creep and fatigue durability demonstrations of a turbine airfoil environmental barrier coating system, consisting of an advanced HfO<sub>2</sub>-rare earth silicate and (Nd,Yb,Al)SiO bond coat, on CVI-SMI and CVI-PIP SiC/SiC CMCs in high heat flux test conditions.

## Summary

High temperature ceramics materials are crucial for aerospace applications because of their very unique properties. Advanced ceramics possess high temperature or ultra-high temperature capabilities, low density, high temperature creep rupture strengths, as well as excellent oxidation and corrosion resistance. Engineered ceramic structural materials are continued to be a main focus for advanced propulsion engine and air-vehicle structural applications because of the ever-increasing needs for efficiency and higher temperature operations.

Zirconia (ZrO<sub>2</sub>) based thermal barrier coatings have been among the most successful applications of modern ceramic materials. Thermal barrier coating systems of ZrO<sub>2</sub>-(6-8)wt% Y<sub>2</sub>O<sub>3</sub>, along with the improvements of nickel-based single crystal superalloy and bond coat technologies, have revolutionized turbine engine industries. Advanced low conductivity multicomponent ZrO<sub>2</sub>-9.5wt% Y<sub>2</sub>O<sub>3</sub>-5.6Yb<sub>2</sub>O<sub>3</sub>-5.2Gd<sub>2</sub>O<sub>3</sub>, and rare earth zirconate (such as Gd<sub>2</sub>Zr<sub>2</sub>O<sub>7</sub> and Sm<sub>2</sub>Zr<sub>2</sub>O<sub>7</sub>), have also been incorporated into engine applications. TBCs with approximately 100 to 150 μm thickness have provided a temperature reduction up to 100 °C for high pressure turbine airfoils, with further advancement towards 200 °C temperature reductions when low conductivity TBCs are implemented. The durability and reliability of turbine engine hot-section components have also been significantly improved largely due to the advances in high stability, high toughness and high strength top coats and bond coats.

Ceramic thermal and environmental barrier coatings have been successfully developed and implemented for protecting emerging SiC/SiC ceramic matrix composite turbine engine components in high temperatures combustion environments. Fundamental degradation mechanisms have been extensively studied due to the stability concerns of the volatile SiO<sub>2</sub> scales for the Si-based ceramics and silicate-based environmental barrier coatings in turbine engine combustion moisture environments. Environmental barrier coating materials, including BASA, mullite, rare earth silicates, rare earth aluminate silicates, and hafnium-rare earth silicates have been developed to provide up to additional

300 °C temperature capability over the current state-of-the-art thermal barrier coating systems. Advanced hafnia – silicon and rare earth – silicon, rare earth – hafnium – silicon based bond coats with controlled oxygen activities have also been developed for 1482°C temperature capable turbine airfoil environmental barrier coating systems.

SiC CMCs reinforced by continuous, polycrystalline high strength SiC fibers are another revolutionary applications of engineered ceramic materials. The turbine engine performance with the CMC components has benefited largely from the materials high temperature capability and low density, thus allowing the design exceeding 200 °C temperature increases compared with nickel base superalloys with significantly reduced cooling. The weight reductions realized by applying SiC/SiC CMCs to engine rotating components can further reduce the design complexity and weight of engine structures. The development and implementation of commercial grades prepreg – MI and CVI-SMI SiC/SiC CMCs have achieved the temperature capability of 1316 °C, while the future SiC/SiC CMC materials are being developed to be capable of 1482 °C when advanced SiC fibers, 3-D fiber architectures and matrix materials are incorporated.

Although ceramic materials have many attributes for high temperature and ultra-high temperature applications, the applications have been limited to less critical components due to their relatively low toughness, low damage tolerance, large variability in their mechanical properties. Complex environmental effects on component design and durability are less understood in thermal gradient and fatigue operating conditions. Advances in testing, modeling and validation methodologies in combined high-heat-flux, simulated thermal gradient environment and fatigue conditions will significantly facilitate the developments of design databases and simulation tools. The understanding of ceramic material characteristics, their underlying degradation mechanisms and interactions will help revolutionize the component design methodologies and component life prediction.

## References

1. R.A. Miller, *Thermal Barrier Coatings for Superalloys*, Philadelphia: TMS, 1980.
2. R.A. Miller, “Current Status of Thermal Barrier Coatings,” *Surface and Coatings Technology*, vol. 30, pp. 1-11, 1987.
3. D. Zhu and R.A. Miller, “Thermal-Barrier Coatings for Advanced Gas-Turbine Engines,” *MRS Bulletin*, vol. 25, no. 7, pp. 43-47, 2000.
4. N.P. Padture, M. Gell and E.H. Jordan, “Thermal-Barrier Coatings for Advanced Gas-Turbine Engines,” *Science*, vol. 296, no. 5566, pp. 280-284, 2002.
5. D.R. Clarke and C.G. Levi, “Materials Design for the Next Generation Thermal Barrier Coatings,” *Annu. Rev. Mater. Res.* 2003, vol. 33, pp. 383-417.
6. C.G. Levi, “Emerging Materials and Processes for Thermal Barrier Coatings,” *Current Opinion in Solid State and materials Science*, vol. 8, pp. 77-91, 2004.
7. I. Spitsberg and J. Steibel, “Thermal and Environmental Barrier Coatings for SiC/SiC CMCs in Aircraft Engine Applications,” *International Journal of Applied Ceramic Technology*, pp. 291-301, 2004.
8. N.P. Padture, “Advanced Structural Ceramics in Aerospace Propulsion,” *Nature Materials*, pp. 804-809, 2016.
9. R. Darolia, “Thermal Barrier Coatings technology: Critical Review, Progress Update, Remaining Challenges and Prospects,” *International Materials Reviews*, pp. 315-348, 2013.
10. R.A. Miller, “Thermal Barrier Coatings for Aircraft Engines: History and Directions,” *Journal of Thermal Spray Technology*, pp. 35-41, 1997.

11. A.G. Evans, D.R. Clarke and C.G. Levi, "The Influence of Oxides on the Performance of Advanced Gas Turbines," *Journal of the European Ceramic Society*, vol. 28, pp. 1405-1419, 2008.
12. R.S. Lima, D. Zhu and L. Li, *Thermal and Environmental Barrier Coatings*, vol. 5A, ASM International, 2013.
13. R.A. Miller, J.L. Smialek and R.G. Garlick, *Phase Stability in Plasma Sprayed Partially Stabilized Zirconia-Yttria*, vol. 3, A. H. H. a. L. W. Hobbs, Ed., Cleveland, OH: The American Ceramic Society, 1982, pp. 242-253.
14. R. Talor, J.R. Brandon and P. Morerel, "Microstructure, Composition and Property Relationships of Plasma Sprayed Thermal barrier Coatings," *Surface and Coatings Technology*, vol. 50, pp. 141-149, 1992.
15. S. Stecura, "Effects of Compositional Changes on the Performance of a Thermal Barrier Coating System," NASA TM-78976, 1978.
16. C. Mercer, J.R. Williams, D.R. Clarke and A.G. Evans, "On a Ferroelastic Mechanism Governing the Toughness of Metastable Tetragonal-Prime (t') Yttria-Stabilized Zirconia," *Proceedings of the Royal Society A*, vol. 463, pp. 1393-1408, 2007.
17. D. Zhu and R.A. Miller, "Sintering and Creep Behavior of Plasma Sprayed Zirconia- and Hafnia-Based Thermal Barrier Coatings," *Surface and Coatings Technology*, vols. 108-109, pp. 114-120, 1998.
18. D. Zhu, R.A. Miller, B.A. Nagaraj and R.W. Bruce, "Thermal Conductivity of EB-PVD Thermal barrier Coatings Evaluated by a Steady-State Laser heat Flux Technique," *Surface and Coatings Technology*, vol. 138, pp. 1-8, 2001.
19. R. Vassen, X. Cao, F. Tietz, D. Basu and D. Stover, "Zirconates as New Materials for Thermal Barrier Coatings," *Journal of the American Ceramic Society*, vol. 83, no. 8, pp. 2023-2028, 2000.
20. J. Wu, X. Wei, N.P. Padture, P.G. Klemens, M. Gell, E. Garcia, P. Miranzo and M.I. Osendi, "Low-Thermal-Conductivity Rare-Earth Zirconates for Potential Thermal-Barrier-Coating Applications," *Journal of American Ceramic Society*, vol. 85, no. 12, pp. 3031-3035, 2002.
21. J.R. Nicholls, K.J. Lawson, A. Johnstone and D.S. Rickerby, "Methods to Reduce the Thermal Conductivity of EB-PVD TBCs," *Surface and Coatings Technology*, vols. 151-152, pp. 383-391, 2002.
22. R. Gadow and M. Lischka, "Lanthanum Hexaaluminate - Novel Thermal Barrier Coatings for Gas Turbine Applications - Materials and Process Development," *Surface and Coatings Technology*, vols. 151-152, pp. 392-399, 2002.
23. D. Zhu and R.A. Miller, "Development of Advanced Low Conductivity Thermal Barrier Coatings," *International Journal of Applied Ceramics*, pp. 86-94, 2004.
24. D. Zhu and R.A. Miller, "Advanced Low Conductivity Thermal Barrier Coatings: Performance and Future Directions," in *35th International Conference on Metallurgical Coatings and Thin Films (ICMCTF 2008)*, San Diego, CA, 2008.
25. Oerlikon Metco, *Thermal Spray Materials Guide*, Westbury, NY, 2017.
26. Praxair Surface Technologies, *Powder Solution catalog*, Indianapolis, IN: Praxair, 2017.
27. R. Vassen, X. Cao, F. Tietz, D. Basu and D. Stover, "Zirconates as New Materials for Thermal Barrier Coatings," *Journal of American Ceramic Society*, vol. 83, no. 8, pp. 2023-2028, 2000.
28. J. Hutchinson and A. G. Evans, "On the Delamination of Thermal Barrier Coatings in a Thermal Gradient," *Surface and Coatings Technology*, vol. 149, pp. 179-184, 2002.
29. J.L. Smialek, "Compiled Furnace Cyclic Lives of EB-PVD Thermal Barrier Coatings," *Surface and Coatings Technologies*, vol. 276, pp. 31-38, 2015.

30. R.G. Wellman and J.R. Nicholls, "A Review of the Erosion of Thermal Barrier Coatings," *J. Phys. D: Appl. Phys.*, vol. 40, pp. R293-R305, 2007.
31. D. Zhu, R.A. Miller and M.A. Kuczarski, "Development and Life Prediction of Erosion Resistant Turbine Low Thermal Conductivity Thermal Barrier Coatings," NASA/TM—2010-215669, 2010.
32. D. Zhu, R.A. Miller and M.A. Kuczarski, "Design and Performance Optimizations of Advanced Low Conductivity Thermal Barrier Coatings for Rotorcraft Engines," NASA/TM—2012-217138, 2012.
33. A. Zisis and N. Fleck, "Mechanisms of Elastodynamic Erosion of Electron-Beam Thermal Barrier Coatings," *Int. J. Mat. Res.*, vol. 98, pp. 1196-1202, 2007.
34. C.G. Levi, M.-H. V.-S. John Hutchinson and C.A. Johnson, "Environmental Degradation of Thermal Barrier Coatings by Molten Deposits," *MRS Bulletin*, vol. 37, pp. 932-941, 2012.
35. G.C.C. Costa, W.A. Acosta, D. Zhu and A. Ghoshal, "Thermochemistry of Calcium-Magnesium-Aluminum-Silicate (CMAS) and Components of Advanced Thermal and Environmental Barrier Coating Systems," NASA/TM—2017-219512, 2017.
36. D. Zhu, D.S. Fox and R.A. Miller, "Thermal and Environmental Barrier Coatings for Advanced Propulsion Engines," in *48th AIAA/ASME/ASCE/AHS/ASC Structures, Structure Dynamics, Materials Conference*, Honolulu, HI, 2007.
37. J.A. DiCralo, "Advances in SiC/SiC Composites for Aero-Propulsion," NASA/TM—2013-27889, 2013.
38. E.J. Opila and R. Hann, "Paralinear Oxidation of CVD SiC in Water Vapor," *Journal of American Ceramic Society*, vol. 80, no. 1, pp. 197-205, 1997.
39. R. C. Robinson and J. L. Smialek, "SiC recession Caused by SiO<sub>2</sub> Scale Volatility under Combustion Conditions: I, Experimental Results and Empirical Model," *Journal of American Ceramic Society*, vol. 82, no. 7, pp. 1817-1825, 1999.
40. D. Zhu, B.A. Sakowski and C. Fisher, "Film Cooled Recession of SiC/SiC Ceramic Matrix Composites: Test Development, CFD Modeling and Experimental Observations," in *41st International Conference on Metallurgical Coatings and Thin Films*, San Diego, CA, 2014.
41. K.N. Lee, "Current Status of Environmental Barrier Coatings for Si-Based Ceramics," *Surface and Coatings Technology*, Vols. 133-134, pp. 1-7, 2000.
42. K.N. Lee, *Environmental Barrier Coatings for SiC/SiC*, Hoboken, NJ, USA: John Wiley & Sons, Inc., 2014.
43. D. Zhu, *Advanced Environmental Barrier Coatings for SiC/SiC Ceramic Matrix Composite Turbine Components*, Hoboken, NJ, USA: John Wiley & Sons, Inc., 2016.
44. G.S. Gorman and K.L. Luthra, "Melta Infiltrated Ceramic Matrix Composites for Shrouds and Combustor Liners of Advanced Industrial Turbines," *Advanced Materials for Advanced Industrial Gas Turbines (AMAIGT) Program Final Report*, December 2010.
45. M.V. Roode, J. Price, J. Kimmel, N. Miriyala, D. Leroux, A. Fahme and K. Smith, "Ceramic Matrix Composite Combustor Liners: A Summary of Field Evaluations," *Journal of Engineering for Gas Turbines and Power*, vol. 129, no. 1, pp. 21-30, 2007.
46. N. Miriyala and J.R. Price, "The evaluation of CFCC Liners after Field Engine Testing in Gas Turbine-II," in *ASME Turbo Expo 2000: Power for Land, Sea, and Air*, ASME 2000-GT-648, Munich, Germany, 2000.
47. K.N. Lee, D.S. Fox, J.I. Eldridge, D. Zhu, R.C. Robinson, N.P. Bansal and R.A. Miller, "Upper Temperature Limit of Environmental Barrier Coatings Based on Mullite and BSAS," *Journal of the American Ceramic Society*, vol. 86, no. 8, pp. 1290-1306, 2003.

48. D. Zhu, K. N. Lee and R. A. Miller, "Thermal Conductivity and Thermal Gradient Cyclic Behavior of Refractory Silicate Coatings on SiC/SiC Ceramic Matrix Composites," *Ceram. Eng. Sci. Proc.*, vol. 22, pp. 443-452, 2001.
49. D. Zhu, S.R. Choi, J.I. Eldridge, K.N. Lee and R.A. Miller, "Surface Cracking and Interface Reaction Associated Delamination Failure of Thermal and Environmental Barrier Coatings," *Ceram. Eng. Sci. Proc.*, vol. 23, pp. 469-475, 2003.
50. K.N. Lee, D.S. Fox and N. Bansal, "Rare Earth Silicate Environmental Barrier Coatings for SiC/SiC Composites and Si<sub>3</sub>N<sub>4</sub> Ceramics," *Journal of the European Ceramic Society*, vol. 25, pp. 1705-1715, 2005.
51. G.C.C. Costa and N.S. Jacobson "Mass spectrometric measurements of the silica activity in the Yb<sub>2</sub>O<sub>3</sub>-SiO<sub>2</sub> system and implications to assess the degradation of silicate-based coatings in combustion environments," *Journal of the European Ceramic Society*, vol. 35, no. 15, pp. 4259-4267, 2015.
52. D. Zhu, N.P. Bansal and R.A. Miller, "Thermal Conductivity and Stability of HfO<sub>2</sub>-Y<sub>2</sub>O<sub>3</sub> and La<sub>2</sub>Zr<sub>2</sub>O<sub>7</sub> Evaluated for 1650°C Thermal/Environmental Barrier Coating Applications," in *Advances in Ceramic Matrix Composites IX*, John Wiley & Sons, Inc., 2004, pp. 341-343.
53. D. Zhu, "NASA's Advanced Environmental Barrier Coatings Development for SiC/SiC Ceramic Matrix Composites: Understanding Calcium Magnesium Alumino-Silicate (CMAS) Degradations and Resistance," in *Thermal Barrier Coatings IV Conference: An ECI Conference Series*, Irsee; Germany, 22-27 June, 2014.
54. N.L. Ahlborg and D. Zhu, "Calcium Magnesium Alumino-Silicate (CMAS) Reactions and Degradation Mechanisms of Advanced Environmental Barrier Coatings," *Surface and Coatings Technology*, vol. 237, pp. 79-87, 2013.
55. D.L. Poerschke, J.V. Sluytman, K. Wong and C. Levi, "Thermochemical Compatibility of Ytterbia-(Hafnia/Silica) Multilayers for Environmental Barrier Coatings," *Acta Materialia*, vol. 61, no. 18, pp. 6743-6755, 2013.
56. D.L. Poerschke, G.E. Seward and C.G. Levi, "Influence of Yb:Hf ratio on ytterbium hafnate/molten silicate (CMAS) reactivity," *Journal of the American Ceramic Society*, vol. 99, pp. 651-659, 2016.
57. D. Zhu and J.B. Hurst, "Advanced High Temperature and Fatigue Resistant Environmental Barrier Coating Bond Coat Systems For SiC/SiC Ceramic Matrix Composites." US Patent US 13/923,450, 21 June 2013.
58. S. Kitaoka, T. Matsudaira, D. Yokoe, T. Kato and M. Takata, "Oxygen Permeation Mechanism in Polycrystalline Mullite at High Temperatures," *Journal of the American Ceramic Society*, vol. 100, no. 7, p. 3217-3226, 2017.
59. M. Wada, T. Matsudaira, N. Kawashima, S. Kitaoka and M. Takata, "Mass Transfer in Polycrystalline Ytterbium Disilicate Under Oxygen Potential Gradients at High Temperatures," *Acta Materialia*, vol. 15, pp. 372-381, 2017.
60. D. Zhu, B. Harder, J.B. Hurst, G.C.C. Costa, R. Bhatt and D.S. Fox, "Development of Advanced Environmental Barrier Coatings for SiC/SiC Ceramic matrix Composites: Path toward 2700 °F Temperature Capability and Beyond," in *41 Annual Conference on Composites, Materials and Structures*, Cocoa Beach, FL, 2017.
61. D. Zhu and J.B. Hurst, "Advanced High Temperature Environmental Barrier Coating for SiC/SiC Ceramic Matrix Composites". US Patent Patent Application Serial No.: 15/625,277, 2017.
62. D. Sacksteder, D. Waters and D. Zhu, "Oxidation Study of Ultra High Temperature Ceramic Coatings Based on HfSiCN," in *Ceramic Engineering and Science proceedings*, Hoboken, NJ, John Wiley and Sons, Inc., 2019. Also NASA/TM—2018-219789, April 2018.

63. M.C. Halbig, M.H. Jaskowiak, J.D. Kiser and D. Zhu, "Evaluation of Ceramic Matrix Composite Technology for Aircraft Turbine Engine Applications, AIAA 2013-0539," in *51st AIAA Aerospace Sciences Meeting including the New Horizons Forum and Aerospace Exposition, Aerospace Sciences Meetings*, Grapevine, TX, January 7-10, 2013.
64. D. Zhu, J.B. Hurst and M.H. Jaskowiak, "Advanced Environmental Barrier Coating Development and Validation for SiC/SiC Ceramic Matrix Composite Turbine Engine Components," in *36th Annual Conference on Composites, Materials, and Structures*, Cocoa Beach, FL, 2012.
65. D. Brewer, "HSR/EPM Combustor Materials Development Program," *Materials Science and Engineering*, vol. A261, pp. 284-291, 1999.
66. G.S. Gorman and K.L. Luthra, "Silicon Melt-Infiltrated Ceramic Composites (HiPerCom)," in *Handbook of Ceramic Composites*, Boston, MA, Kluwer Academic Publishers, 2005, pp. 99-115.
67. K. Luthra, "Emerging Applications and Challenges in using Ceramics at General Electric," in *Ceramic Leadership Summit 2011*, Baltimore, MD, August 1-3, 2011.
68. J.A. DiCarlo, "SiC Fiber Creep and Rupture Models for Understanding CMC Behavior above 1400 °C," in *Workshop on the Design of Ceramic-Fiber Based Composites for Service Above 1400 °C*, Boulder, CO, June 2012.
69. J.A. DiCarlo, N.S. Jacobson, M. Lizcano and R. Bhatt, "Ultra High Temperature (UHT) SiC Fiber (Phase II)," NASA/TM—2015-218883, 2015.
70. J. DiCarlo and R. Bhatt, "Modeling SiC/SiC Creep Rupture Behavior from 2400 to 3000 °F," in *35th Annual Conference on Composites, materials, and Structures*, Coca Beach, FL, January 24-27, 2011.
71. R. Bhatt, J.A. DiCarlo and J.D. Kiser, "Tensile and Creep properties of Hybrid CVI-PIP SiC/SiC Composites at High Temperatures in Air," in *36th Annual Conference on Composites, materials, and Structures*, Cocoa Beach, FL, January 23-26, 2012.
72. D. Zhu, R. Bhatt and B. Harder, "Combined Thermomechanical and Environmental Durability of Environmental Barrier Coating Systems on SiC/SiC Ceramic Matrix Composites," in *9th International Conference on High Temperature Ceramic Matrix Composites (HTCMC-9)*, Toronto, Canada, 2016.
73. D. Zhu, "Development of Durable Ceramic Matrix Composite Turbine Components for Advanced Propulsion Engine Systems," in *8th Pacific Rim Conference on Ceramic and Glass Technology*, Vancouver, British Columbia, Canada, 2009.





